SRF CAVITY DETUNING CHARACTERIZATION BY CONTINUOUS WAVELET TRANSFORM: A TIME-FREQUENCY ANALYSIS*

J. S. Romero[2], P. Echevarria[1], A. Neumann[1], A. Ushakov[1], C. M. Cuesta[2], J. Knobloch[1,3]
[1]Helmholtz-Zentrum Berlin für Materialien und Energie, Berlin, Germany
[2]University of the Basque Country, Leioa, Spain
[3]University of Siegen, Siegen, Germany

Abstract

Sustainability is a key issue for both current and future particle accelerators. Superconducting RF cavities with high loaded quality factors play an important role in not only lowering the energy demands of particle accelerators but also the initial investment in RF amplifiers. But the narrow bandwidth associated with this high loaded quality, makes the need to minimize cavity detuning critical to maintain stable and efficient operation. In this context, characterization of microphonics detuning is essential, as it is a major error source, for implementation of effective mitigation schemes to reduce peak and rms RF power requirements.

Here we analyze SRF cavity detuning using the Continuous Wavelet Transform (CWT). Unlike conventional Fourier-based approaches, the CWT enables localized time-frequency decomposition, making it well-suited for identifying transient features that influence cavity behavior. Applying the CWT to measured detuning signals from a TESLA cavity at HoBiCaT testing facility at Helmholtz-Zentrum Berlin allows us to identify dominant detuning frequencies and track their evolution over time. The resulting time-frequency maps offer a more comprehensive understanding of the underlying mechanical environment and can support the development of more robust detuning mitigation and compensation strategies for SRF systems.

INTRODUCTION

Particle accelerators are not immune to the current political, social, and economic situation. In this regard, both climate change and rising energy costs make sustainability a key consideration in both existing accelerators and future projects, [1]. Different research projects funded by the European Union [2, 3] are studying different strategies to tackle this issue. One of the tasks in [2] is trying to find paths to save energy from the RF power. More specifically in the case of low beam loading applications, as it is also stated in the European Roadmap for Particle Physics, [4], one major challenge due to the very small intrinsic cavity bandwidth, are small mechanical vibrations known as microphonics.

While active compensation via the cavity tuner is an open field of research, [5–10], passive measures like cryoplant operation optimization, vacuum pumps isolation, etc., should always be considered in the first place, [11]. And for these measures to be effective, a proper characterization of the microphonics is fundamental.

The analysis of detuning signals requires tools capable of capturing time-dependent spectral variations. Classical Fourier analysis provides a global description that does not retain temporal information. To address this limitation, extensions such as the short-time Fourier transform (STFT) introduce time localization by applying the transform over sliding windows. However, the STFT uses a fixed window length, leading to a trade-off between time and frequency resolution that remains constant across all frequencies. This can be limiting for cavity detuning signals, where slow drifts and fast transient events may coexist.

For this reason, the continuous wavelet transform (CWT) is used in this work, as it provides a time-frequency representation with adaptive resolution, [12].The wavelet transform of a continuous time signal, $x(t)$, is defined as

$$T(a,b) = \frac{1}{\sqrt{a}} \int_{-\infty}^{\infty} x(t) \psi^* \left(\frac{t-b}{a} \right) \mathrm{d}t, \tag{1}$$

where $\psi(t)^*$ is the complex conjugate of the wavelet function $\psi(t)$, a is the scale parameter (inversely related to frequency), and b is the time-shift parameter of the wavelet. This formulation represents the signal as a superposition of time-localized contributions at different scales and positions.

Different choices of the wavelet function $\psi(t)$ emphasize specific signal features; for instance, commonly used wavelets such as Morlet or Mexican hat offer different compromise between time and frequency localization.

In this work, the complex Morlet wavelet is used and is given by the following equation

$$\psi(t) = \frac{1}{\sqrt{\pi B}} e^{2\pi i F t} e^{-t^2/B} \tag{2}$$

as it offers a well-defined central frequency and is particularly suitable for analyzing oscillatory signals. The specific parameters used are $F = 1.5$ and $B = 2.5$, where F is the center frequency and B is the bandwidth parameter.

The results shown in this paper were obtained in the HoBiCaT facility at HZB, [13, 14], using a TESLA cavity but also briefly during the first beam commissioning of SEALab's photoinjector, [15, 16].

EXPERIMENT SETUP AND RESULTS

In order to measure the detuning of a cavity, the equation $\Delta f(t) = \frac{f_0}{2Q_L} \tan(\Delta\Phi(t))$ can be used, where $\Delta f(t)$ is the detuning, f_0 the cavity's fundamental mode's frequency,

* Funded by the EU Horizon Europe program grant N. 101131435 and partly funded by the Global Training Program, an initiative of Basque Trade and Investment, SPRI and Basque Government (Spain).

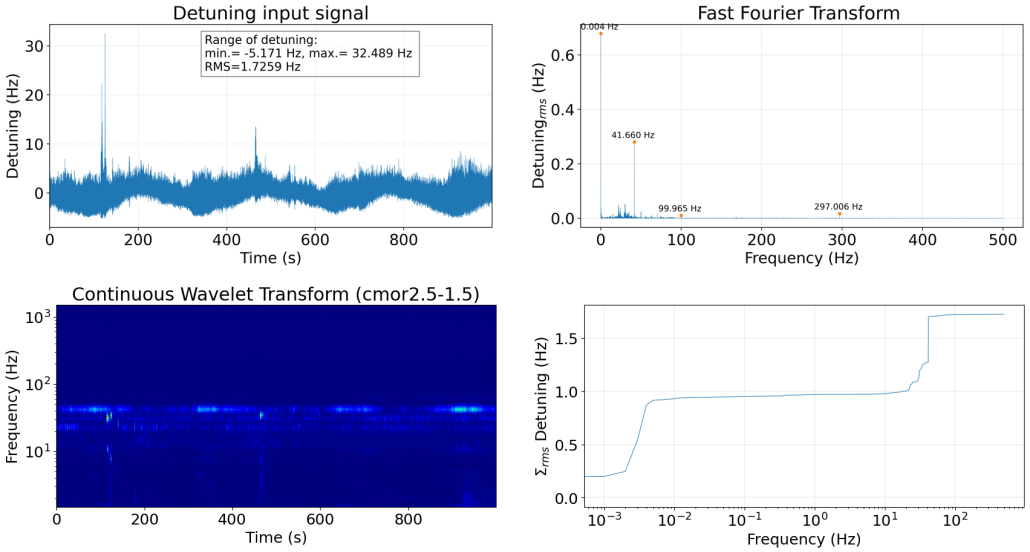

Figure 1: Detuning analysis at $Q_L = 4.5 \times 10^7$: raw detuning signal (top left), FFT spectrum (top right), CWT scalogram (bottom left), and integrated RMS detuning spectrum (bottom right)

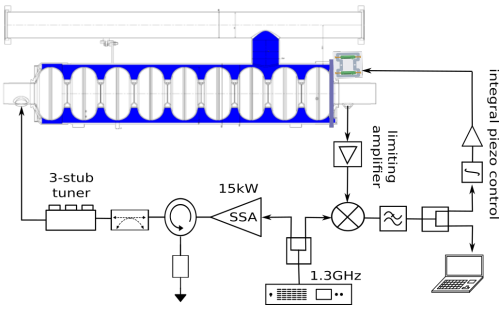

Figure 2: Experiment setup at HoBiCaT for detuning measurements.

Q_L the effective loaded quality factor and $\Phi(t)$ the phase difference between the forward and transmitted signals.

Figure 2 shows the layout of the measurements setup: a signal generator sends the 1.3GHz signal to a 15kW Solid State Amplifier (SSA) which is followed by a motorized three-stub tuner to externally modify the Q_L. Then, the transmitted signal from the pickup antenna is leveled and amplified and mixed with the forward signal. The result is low-pass filtered, acquired and stored. A slow piezoactuator integral control was also added to compensate for slow drifts, allowing capturing longer time windows.

Unfortunately, a technical problem with a getter pump caused a vacuum event in the cavity and further on the radiation on-set field was around 5MV/m. Detuning signals were acquired under continuous wave (CW) operation at two different loaded quality factors, $Q_L = 4.5 \times 10^7$ and $Q_L = 8.6 \times 10^6$, and over a time window of approximately 16 minutes each. Figures 1 and 3 show the analysis for both Q_L values.

At $Q_L = 4.5 \times 10^7$ (Fig. 1), the cavity bandwidth narrows to approximately 29 Hz, making the detuning signal highly sensitive to any mechanical perturbation. The signal spans from -5.171 Hz to 32.489 Hz and exhibits two sharp transient detuning events at approximately $t = 120$ s and $t = 480$ s, which appear as short-lived broadband bursts in the time-frequency map. The FFT is dominated by a component near 0 Hz, reflecting slow non-stationary drifts whose timescale is comparable to the measurement window. A component at 41.660 Hz and weaker ones at 99.965 and 297.006 Hz are also identified.

At $Q_L = 8.6 \times 10^6$ (Fig. 3), the wider cavity bandwidth of approximately 151 Hz results in a less sensitive detuning signal, with a range of ± 10 Hz and no sharp transient events. The reduced influence of slow drifts in this measurement is reflected in the FFT, where a richer microphonics spectrum becomes visible, with a dominant peak at 41.6 Hz and additional components at 100, 168.3, 217.7 and 297 Hz. The CWT confirms these as persistent narrowband features continuously present throughout the measurement. The integrated RMS spectrum shows a gradual accumulation of detuning contributions with clear steps at approximately 10 Hz and 40 Hz, reaching a total RMS detuning of approximately 1.9 Hz. The RMS remains comparable, as it is dominated by persistent rather than transient contributions.

The component at 297 Hz, present in both HoBiCaT measurements, is consistent with the known operating frequency of the helium pumping system at HoBiCaT. Meanwhile, the origin of the 41.6 Hz component also present in both measuremnts is a known mechanical resonance mode, [10].

A similar setup as the one explained above was also used during the first SEALab's photoinjector commissioning, excluding the slow integral control. Figure 4 shows the corresponding analysis of the detuning signal, where impact-like detunings were recorded, these appear in the CWT as localized bursts. While the FFT identifies dominant components at 100 Hz and 278.8 Hz, with weaker contributions at 1017.3 Hz and 1320.7 Hz, the CWT reveals that some components are not continuously present and only appear only during the burst activity. A persistent low-frequency component near 10 Hz is also observed throughout the full

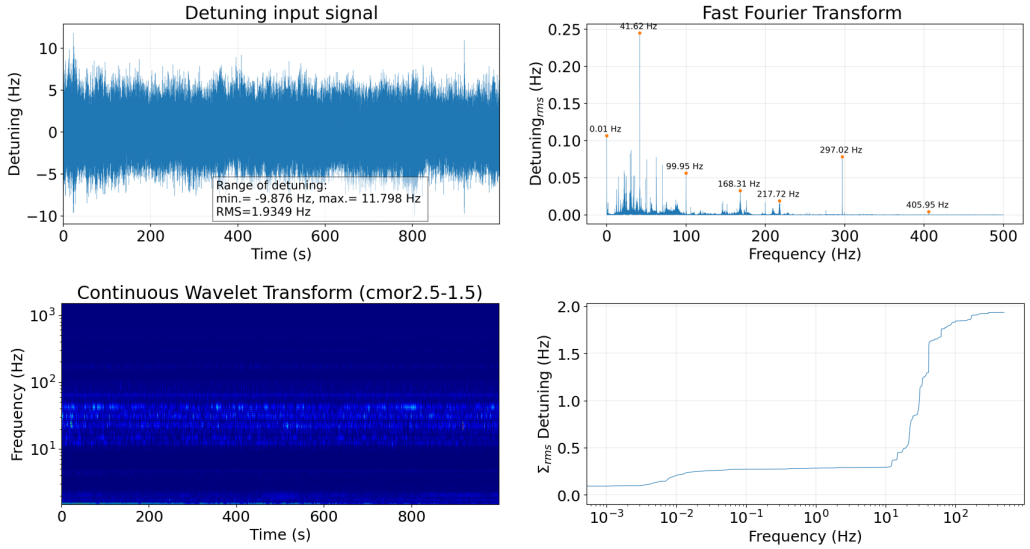

Figure 3: Detuning analysis at $Q_L = 8.6 \times 10^6$: raw detuning signal (top left), FFT spectrum (top right), CWT scalogram (bottom left), and integrated RMS detuning spectrum (bottom right)

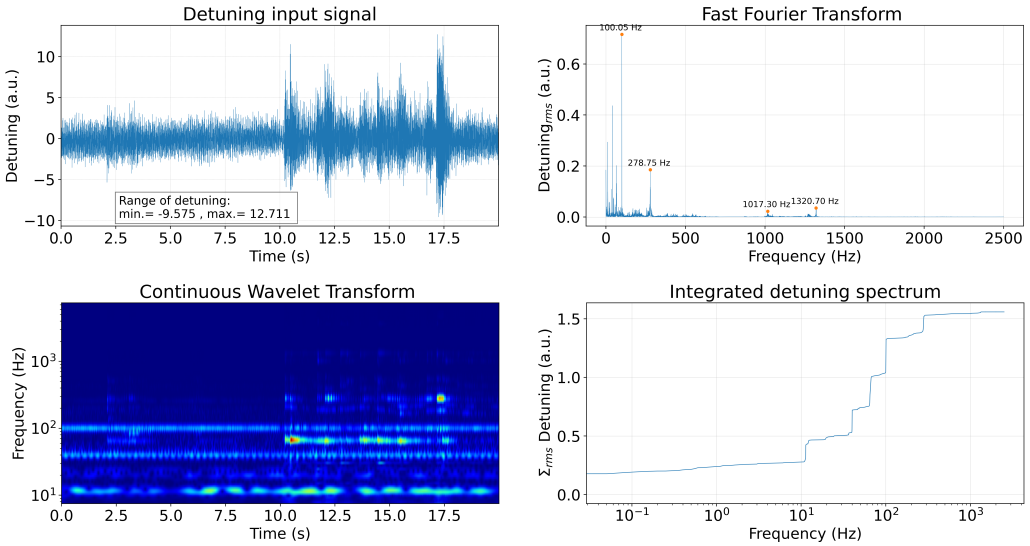

Figure 4: Detuning analysis at SEALab's photoinjector at $Q_L = 2.95 \times 10^7$: raw detuning signal (top left), FFT spectrum (top right), CWT scalogram (bottom left), and integrated RMS detuning spectrum (bottom right)

measurement window. The integrated RMS spectrum confirms dominant contributions at ~ 10 Hz and 100 Hz, with an additional step at ~ 1000 Hz associated with the high-frequency transient content. It is suspected that this kind of events are caused by the cryogenic system and and this case illustrates particularly well the capability of the CWT to resolve transient microphonic effects that would otherwise be masked in a spectral analysis.

CONCLUSIONS

In this work, the CWT has been applied to SRF cavity detuning signals measured in a TESLA cavity at HoBiCaT and in SEALab's photoinjector. The results demonstrate that the CWT provides a more complete characterization of microphonics than conventional Fourier-based approaches, particularly in the presence of transient and non-stationary detuning events. While the FFT identifies the frequency content of persistent components, it fails to capture the temporal evolution of transient bursts, which appear clearly as localized features in the CWT time-frequency maps. This was especially evident in the data measured at SEALab, where impact-like detuning events were shown to activate a 100 Hz component only during the burst activity.

Future work will focus on improving the scalogram contrast through signal preprocessing prior to the CWT computation, and on extending the analysis to longer datasets and different operating conditions. The use of accelerometers in combination with the CWT is also planned to correlate mechanical vibration sources with the observed detuning features, supporting the development of more effective microphonics mitigation strategies.

REFERENCES

[1] M. Benedikt *et al.*, "Future Circular Collider Feasibility Study Report", CERN, Geneva, Rep. 17, 2025. doi:10.17181/CERN.I26X.V4VF

[2] iSAS: Innovate for Sustainable Accelerating Systems, https://isas.ijclab.in2p3.fr/

[3] RF2.0 Research Facility: towards a more energy-efficient and sustainable path, https://rf20.eu/

[4] C. Adolphsen *et al.*, *European Strategy for Particle Physics - Accelerator R&D Roadmap*. 2022. doi:10.23731/CYRM-2022-001

[5] Z. A. Conway and M. Liepe, "Fast Piezoelectric Actuator Control of Microphonics in the CW Cornell ERL Injector Cryomodule", in *Proc. PAC'09*, Vancouver, Canada, May 2009, paper TU5PFP043, pp. 918–920. https://jacow.org/PAC2009/papers/TU5PFP043.pdf

[6] A. Neumann, W. Anders, O. Kugeler, and J. Knobloch, "Analysis and active compensation of microphonics in continuous wave narrow-bandwidth superconducting cavities", *Phys. Rev. ST Accel. Beams*, vol. 13, no. 8, p. 082001, Aug. 2010. doi:10.1103/PhysRevSTAB.13.082001

[7] J. P. Holzbauer *et al.*, "Active Microphonics Compensation for LCLS-II", in *Proc. IPAC'18*, Vancouver, Canada, Apr.-May 2018, pp. 2687–2689. doi:10.18429/JACoW-IPAC2018-WEPML007

[8] N. Banerjee, G. Hoffstaetter, M. Liepe, P. Quigley, and Z. Zhou, "Active suppression of microphonics detuning in high Q_L cavities", *Phys. Rev. Accel. Beams*, vol. 22, no. 5, p. 052002, May 2019. doi:10.1103/PhysRevAccelBeams.22.052002

[9] A. Bellandi, J. Branlard, H. Schlarb, and C. Schmidt, "Feedforward resonance control for the european x-ray free electron laser high duty cycle upgrade", *Frontiers in Physics*, vol. Volume 11 - 2023, 2023. doi:10.3389/fphy.2023.1170175

[10] A. Elejaga, J. Jugo, P. Echevarria, A. Neumann, A. Ushakov, and J. Knobloch, "Experimental testing of a modified active disturbance rejection control for microphonics reduction in a 9-cell tesla superconducting cavity", *Phys. Rev. Accel. Beams*, vol. 27, no. 11, p. 113501, Nov. 2024. doi:10.1103/PhysRevAccelBeams.27.113501

[11] J. P. Holzbauer *et al.*, "Passive Microphonics Mitigation during LCLS-II Cryomodule Testing at Fermilab", in *Proc. IPAC'18*, Vancouver, Canada, Apr.-May 2018, pp. 2668–2670. doi:10.18429/JACoW-IPAC2018-WEPML001

[12] S. Mallat, *A wavelet tour of signal processing*. San Diego: Academic Press, 1999. doi:10.1016/B978-012466606-1/50002-7

[13] J. Knobloch, W. Anders, D. Pflückhahn, and M. Schuster, "HoBiCaT - A Test Facility for Superconducting RF Systems", in *Proc. SRF'03*, Lübeck, Germany, Sep. 2003, paper MOP48, pp. 173–175. https://jacow.org/SRF2003/papers/MOP48.pdf

[14] O. Kugeler, A. Neumann, W. Anders, and J. Knobloch, "Adapting TESLA technology for future cw light sources using HoBiCaT", *Review of Scientific Instruments*, vol. 81, no. 7, p. 074701, Jul. 2010. doi:10.1063/1.3443561

[15] T. Kamps *et al.*, "Accelerator physics experiments at the versatile SRF photoinjector of SEALab", in *Proc. IPAC'23*, Venice, Italy, pp. 2115–2118, Sep. 2023. doi:10.18429/JACoW-IPAC2023-TUPL160

[16] T. Kamps *et al.*, "First beam commissioning of the HZB SRF photoelectron gun", in *Proc. IPAC'25*, Taipei, Taiwan, pp. 1718–1721, Nov. 2025. doi:10.18429/JACoW-IPAC2025-WECN2